3.2 TEN YEAR CLIMATOLOGY OF CAPE OBSERVATIONS EAST OF THE ROCKY MOUNTAINS FROM HYPERSPECTRAL IR SOUNDERS

Jessica Gartzke and R. Knuteson, S. A. Ackerman, W. Feltz, and G. Przybyl
CIMSS/Univ. of Wisconsin, Madison, WI

1. Abstract

High priority must be given to research for Earth remote sensing applications especially relating to severe weather. For example, a climatology of Convective Available Potential Energy (CAPE) is routinely used to characterize convection as having moderate or severe potential. Relating a CAPE climatology to near real time observations from meteorological sensors on new weather satellites is a valuable tool in assessing the risk of severe weather. Satellite data products from AQUA AIRS were used to compute a 10 year climatology for the Southern Great Plains region. CAPE was computed from vertical profiles of pressure, temperature, and dew point temperature from high vertical resolution AIRS soundings (101 levels) using the SHARPpy algorithm used by the National Weather Service Storm Prediction Center. Forecasters could in principle make use of CAPE estimates from operational satellite sounders such as CrIS and IASI on JPSS and METOP platforms during the most unstable daytime period. A goal of this project is to outline a path towards obtaining near-real time hyperspectral satellite soundings of temperature and water vapor from direct broadcast and making these data via the SHARPpy software. A climatology of CAPE on approximately 50 km scales will be presented to demonstrate the usefulness of satellite remote sensing data in characterizing severe storms.

2. Introduction

The ability to measure vertical profiles of water vapor from space at times when ground based upper air soundings are not available can fill an important need in short-range weather prediction. New satellite observations allow for the retrieval of water vapor measurements with higher vertical resolution than was previously available. In order to demonstrate these new data opportunities, it’s important to look at a practical application. Supercell thunderstorm events, like the El Reno, Oklahoma tornado on 31 May 2013, are examples of just how dangerous and unpredictable tornados can be. Fig. 1 demonstrates the severe convection from this disastrous storm. The El Reno case study will be used to illustrate the potential value of satellite soundings. Fig. 2 compares the regional CAPE for the El Reno case study between ECMWF ERA-Interim model fields and NASA AIRS L2 v6 satellite observations. While very similar to each other, there are notable differences in the precise location of the most extreme CAPE values with the satellite observation of peak CAPE slightly west of the model analysis. Note that El Reno is just west of Norman, OK and is where the supercell formed that produced the El Reno tornado. Fig. 3 provides an example comparison of the vertical soundings of temperature and dewpoint temperature at the DOE ARM SGP site (just north of El Reno) at about noon on that day. Note that the radiosonde profile has much higher vertical resolution than either the NWP model or the satellite retrieved profile from AIRS.

National Weather Service (NWS) forecasters are using GOES sounder products for a range of applications, with positive results. These products include estimates of total precipitable water vapor (TPW) and atmospheric stability indices, such as convective available potential energy (CAPE) and lifted index (LI). Infrared observations from geostationary orbit capture the diurnal cycle of surface skin temperature with data collected over the continental United States every hour. These geostationary data can contribute to future warn on forecast approaches (Stensrud 2009) . However, the limited number of infrared spectral channels fundamentally limits the vertical resolution of the existing GOES sounder thermodynamic products.

Unlike the current GOES sounder, new high spectral resolution infrared sensors on polar orbiting weather satellites (POES) can sense the atmospheric boundary layer at specific times of day (about 10:30 am/pm and 1:30 am/pm). For example, the Atmospheric Infrared Sounder (AIRS) has been used to provide quantitative information about the lower atmosphere (Chahine 2006) . Software to process AIRS data in near real-time has been included in the IMAPP direct broadcast software package (Al 2012)(Weisz et al. 2013). Near real-time data assimilation of polar orbiting advanced sounder products into rapid update NWP models has the potential to provide positive impact for future warn on forecasts (Stensrud 2009).

A common goal of the severe storm science community is to obtain accurate information in a timely manner regarding atmospheric stability. This information can be used to communicate predictions of severe weather events. The first objective of this paper is to illustrate the value of advanced polar sounder observations, through the El Reno event using the 1:30 pm polar satellite orbit. The second is to put this event in the context of the climatology of the southern Great Plains and assess the ability of POES satellites to provide reliable stability information. In this paper, a ten year record of upper air sounding profiles from the Department of Energy Atmospheric Radiation Measurement (ARM)

Southern Great Plains (SGP) site was used to create a climatology of Convective Available Potential Energy (CAPE). The seasonal variation in CAPE and dewpoint is shown in Fig. 4. We then look at the ability of satellite observations to characterize the CAPE probability distribution function at the 1:30 am/pm overpass times as a function of distance from the SGP site.

3. Methods

To obtain a statistically useful range of CAPE values in the U.S. southern Great Plains, vertical profiles of pressure, temperature and water vapor were obtained for the time period January 1, 2005 to December 31, 2014 for a region centered on the ARM SGP central facility. The ARM site was chosen for this study because routine radiosonde launches at 6 UTC and 18 UTC are within 1.5 hours of the nominal satellite overpass times of the AQUA satellite. Values of CAPE were computed for each vertical profile using software consistent with that of the NWS Storm Prediction Center (SPC) (Hart, J. A., J. Whistler, R. Lindsay 1999). Only cases with radiosonde profiles having CAPE greater than 50 J/kg were included in the analysis. This threshold was used to eliminate the large number of zero (or small) CAPE values that are not relevant for severe weather. To investigate spatial sampling issues, CAPE values from AIRS and ERA were selected within a radius of 50, 150, and 250 km of the ARM SGP central facility. The selected CAPE values for a time and space region are used to create histograms using a uniform bin size of 50 J/kg. Normalizing by the sum of the histogram creates a probability distribution function (PDF). PDF percentiles at 25, 50, 67, 75, 95 and 99th were tabulated to quantify the characteristics of each CAPE distribution.

To analyze the dependence of CAPE on the vertical resolution of the temperature and water vapor profiles, the radiosonde profiles were smoothed with a vertical boxcar function at width values (1 3 5 7 9 15 21 27 35 41 47 53) of 75 meters per layer. The CAPE computed from the smoothed profile was differenced from the original radiosonde CAPE for each profile.

The following equation defines CAPE (Blanchard, 1998)

$$\text{CAPE}=g\int_{EL}^{LFC}\frac{(T_{v,parcel}-T_{v,env})}{T_{v,env}}\,dz \quad (1)$$

The forecasted parcel is a parcel estimate at the expected time of convection. This paper utilizes the surface parcel method for calculating CAPE. In particular, this study uses the SHARPpy software routines described in Halbert (Halbert et al. 2015). SHARPpy is a python software library that can be used by the research community and is derived from the SHARP software used operationally at the Storm Prediction Center (Hart, J. A., J. Whistler, R. Lindsay 1999).

4. Results

An analysis was performed to understand the ARM radiosonde, ERA, and AIRS CAPE sensitivity to spatial, temporal, vertical, and measurement error.

a. Spatial Sampling Error

For the satellite product, a spatial sampling error can exist when the AIRS profile coincident with the SGP site location is invalid, e.g. overcast, and the closest valid profile is some distance away. To quantify this issue an analysis was created for CAPE values within a radius of the ARM SGP site. The spatial sampling error for the ERA interim can be neglected because the model grid is continuous over the domain of interest; however the ERA was analyzed at the same circular region for consistency with the AIRS analysis. There is no significant spatial sampling error in the AIRS product due to invalid retrievals when using the quality control criteria given in Table 1.

b. Temporal Sampling Error

Temporal sampling error can be an important error in CAPE estimation given the rapid boundary layer changes due to surface heating during the day and cooling after sunset. For this reason, operational radiosondes launched at 0 and 12 UTC (6 am and 6 pm) are not ideal for of assessment of CAPE during mid-day in the SGP region. The ARM SGP site was chosen for this study of AIRS CAPE because research grade radiosondes are launched at 6 and 18 UTC (about midnight and noon local time). The afternoon satellite overpass is at about 1:30 pm (19:30 UTC) with some variation from day to day. The radiosonde launch time and Aqua satellite overpass time difference is typically less than 2 hours. To further minimize this relatively small temporal sampling error, the radiosonde data was interpolated to each Aqua satellite overpass times. The ERA Interim analyses are available only at 0, 6, 12, and 18 UTC. For this study, the 6 and 18 UTC ERA analysis fields are used without time interpolation and thus represent the atmospheric state about 1 to 2 hours prior to the satellite overpass but they are time coincident with the ARM SGP radiosonde launches.

c. Vertical Resolution Error

The ARM radiosondes were used to investigate the dependence of CAPE on vertical resolution of the temperature and moisture sounding. In the ARM product file used for this study, the radiosonde data has been interpolated to 200 height bins with a spacing of 75 meters and two additional bins at 2 m and 30 m. A boxcar smoother was applied to each vertical profile for a range of boxcar full widths and CAPE was recomputed for each smoothed profile. Results are summarized in Fig. 6. There is an 11% reduction in CAPE for a full-width vertical smoothing of 1000 meters. A vertical smoothing of 2000 m causes a reduction in CAPE values of about 18%. AIRS has a reduction of 17% at the 50th percentile which is roughly consistent with the expected vertical resolution of about 2 km for retrieved water vapor profiles inherent to the hyperspectral infrared (Chahine 2006).The ERA model 50th percentile is biased by -23% relative to radiosonde profiles, which may be due to a vertical smoothing inherent in the NWP model, particularly with respect to the vertical layering of water vapor. This is apparent in the dew point profiles of the case study examples shown in Fig. 3.

Vertical smoothing of the radiosonde profiles can occasionally lead to a temporary increase in CAPE values as indicated by the positive outliers. Fig. 7 illustrates the effect of smoothing a profile containing a nocturnal temperature inversion. The surface parcel temperature increases with smoothing in this case, which leads to an increase in the CAPE value computed from the smoothed profile. Investigation of these anomalous cases of increasing CAPE shows they are all profiles at night containing a temperature inversion.

d. Measurement Error

The case study analysis revealed a sensitivity of CAPE to surface parcel temperature and dewpoint temperature, i.e. an error in the surface parcel estimate could cause errors in the computed CAPE. In order to quantify this error, the ARM radiosonde surface temperature and dew point temperature was used as a reference to compute the error in the surface parcel estimates from the closest AIRS retrieved profiles and ERA reanalysis profiles to the ARM SGP launch site. The mean differences are less than 1 °C in each comparison with a standard deviation of about 2 °C; however, this good statistical agreement in the mean disguises an error when CAPE is non-zero. Table 2 shows the result of analyzing the 10-year matchup dataset for the subset of cases with CAPE greater than a minimum cutoff. The most notable feature in Table 2 is how the error in surface dew point changes from near zero for all CAPE values to -2 °C for the subset with CAPE greater than a minimum value of 50 J/kg. This is error is the same for both AIRS and ERA. As the CAPE minimum threshold increases the error grows for both ERA and AIRS with ERA exceeding -5 °C and for AIRS exceeding -7 °C for the CAPE values greater than 2500 J/kg. Surface air temperature error also grows with increasing CAPE but the error is less than half as large as the dew point temperature error. Table 2 shows very similar behavior between ERA and AIRS for CAPE up to 1500 J/Kg. For higher CAPE values, the AIRS bias error exceeds that of ERA although both have equally large standard deviations.

To characterize the extent to which errors in the surface parcel estimates lead to error in the derived CAPE estimates, a correlation coefficient was computed between AIRS and ARM radiosonde for nonzero CAPE values with a range of quality control criteria. Decreasing the AIRS cloud fraction cutoff increases the correlation with ARM radiosondes from 0.35 to 0.5, however the highest correlation (>0.8) is achieved only when the surface dew point of AIRS is within 1 °C of the ARM site radiosonde. This is illustrated in Fig. 8. The left hand panels show the variation with cloud fraction, from < 0.8 to < 0.1, while the right hand panels show the additional effect of restricting the subset to dew point temperature with agreement better than 1 °C. This demonstrates that the scatter in the matchup between AIRS and ARM SGP radiosonde CAPE values is primarily driven by an error in the estimation of the surface parcel dew point temperature. The comparison of the right column of Fig. 8 shows that a high correlation (>0.84) can be obtained even for AIRS cloud fractions up to 0.8 as long as the surface dew point estimate is within 1 degree of the truth. Fig. 8 also shows the comparison of AIRS and ERA with a similar restriction on cloud fraction and surface dew point error. The correlation coefficient between AIRS and ERA increases from 0.37 to 0.88 when the surface dew point temperatures agree to within 1 °C independent of AIRS cloud fraction.

The systematic bias found in the AIRS derived CAPE and the ERA-Interim derived CAPE is consistent with the known reduced vertical resolution of NWP and satellite retrievals compared to radiosondes. However, the scatter in the AIRS and ERA-Interim CAPE values relative to radiosondes was shown to be primarily due to error in the estimate of the surface parcel dew point temperature. To account for this error and develop a correction method, a comparison between ASOS automated surface observations at Ponca City, OK (near the ARM SGP site) and AIRS retrieved surface temperature and dew point was conducted. A time series plot was created to see the seasonal variation in the two sets of data as shown in Fig. 9. When comparing surface temperatures, AIRS is seeing higher temperatures in the winter than ASOS. In summer, when CAPE is high, there is a fair amount of scatter but no bias for AIRS 2 meter temperature as seen in Fig. 10. In contrast, the AIRS estimated dew point is drier than the ASOS estimated dew point by several degrees in the summer. This is consistent with what we found at the ARM site. The next step is to use the ASOS surface temp and dew point in updating the satellite CAPE calculation. Future work includes the use of ASOS surface temperature and dew point observations coincident with AIRS soundings to improve CAPE estimates in near-real time for the continental US east of the Rockies.

5. Discussion

Several authors have validated AIRS retrieved temperature and moisture vertical profiles (Bedka, S., Knuteson, R., Revercomb, H., Tobin, D., & Turner 2010) (Tobin et al. 2006) (Divakarla et al. 2006) (Fetzer et al. 2006). Only a limited study has been published previously on the accuracy of CAPE derived from AIRS profiles relative to radiosondes (Botes et al. 2012). That study commented on the lack of correlation of CAPE derived from AIRS to the CAPE derived from the small number of radiosonde profiles considered, but no explanation was provided for the result. For the current study, a long time series of AIRS and radiosonde matchups was created to characterize the systematic biases and random characteristics of the hyperspectral infrared satellite retrievals. As shown in Fig. 5, the AIRS and ERA CAPE distributions share similar characteristics, including a smaller median value relative to ARM radiosondes. This under-estimate is consistent with the lower vertical resolution of the satellite and NWP products. The relatively poor correlation of AIRS and ERA CAPE with matched ARM SGP radiosondes (0.35 and 0.5, respectively) is explained by an error in estimation of the surface parcel dew point temperature.

6. Conclusion

A comparison of CAPE was made for the U.S. Southern Great Plains region using a combination of DOE ARM radiosondes, ERA model reanalysis fields, and AIRS satellite observations. CAPE estimates were evaluated for spatial, temporal, vertical resolution and measurement errors. Numerical estimates of CAPE are sensitive to the vertical smoothing of the temperature and moisture profile. A vertical smoothing of 1-2 km leads to a reduction in the 50th percentile of CAPE by 10-20 percent. In addition, error in the surface parcel dew point estimate is found to degrade the accuracy of CAPE. For CAPE values greater than 50 J/kg, both AIRS and ERA-Interim surface dew point temperatures are dry by 2 degrees compared to the surface radiosonde observations. This error increases to more than 5 degrees Celsius for CAPE exceeding 2500 J/kg. Improvements of surface parcel dew point temperature can be expected to improve the CAPE estimates derived from both hyperspectral infrared satellite observations and NWP forecasts. This suggests that merging surface station meteorological data and available boundary layer profiling with satellite profiles could greatly improve the utility of the hyperspectral satellite sounding products and the NWP model fields. In conclusion, timely and useful information on the evolution of the vertical structure of the atmosphere is available from the satellite overpasses at 10:30am (EUMETSAT/METOP) and at 1:30pm (NASA Aqua and NOAA/JPSS) and should be exploited for NWS forecasting applications.

7. Acknowledgements

The author wishes to thank Genevieve Burgess for assisting in the acquisition of AIRS products and discussions with Greg Blumberg on the use of the SHARPpy software. We acknowledge the support of NOAA grant NA10NES4400013. In addition, acknowledgment is made for the contribution of Dave Turner for the ARM data obtained from the DOE archive at http://www.archive.arm.gov.

8. References

Al, S. E. T., 2012: Dual-Regression Retrieval Algorithm for Real-Time Processing of Satellite Ultraspectral Radiances. *J. Appl. Meteor. Climatol.*, 1455–1476, doi:10.1175/JAMC-D-11-0173.1.

Bedka, S., Knuteson, R., Revercomb, H., Tobin, D., & Turner, D., 2010: An assessment of the absolute accuracy of the Atmospheric Infrared Sounder v5 precipitable water vapor product at tropical, midlatitude, and arctic ground. *J. Geophys. Res. Atmos.*, 181–202, doi:10.1175/2009JAMC2286.1.

Botes, D., J. R. Mecikalski, and G. J. Jedlovec, 2012: Atmospheric Infrared Sounder (AIRS) sounding evaluation and analysis of the pre-convective environment. *J. Geophys. Res. Atmos. Geophys. Res.,* **117**, 1–22, doi:10.1029/2011JD016996.

Chahine, M. T., 2006: Improving Weather Forecasting and Providing. *Bull. Amer. Meteor. Soc.*, 911–927, doi:10.1175/BAMS-87-7-911.

Divakarla, M. G., C. D. Barnet, M. D. Goldberg, L. M. McMillin, E. Maddy, W. Wolf, L. Zhou, and X. Liu, 2006: Validation of Atmospheric Infrared Sounder temperature and water vapor retrievals with matched radiosonde measurements and forecasts. *J. Geophys. Res. Atmos.*, **111**, 1–20, doi:10.1029/2005JD006116.

Fetzer, E. J., B. H. Lambrigtsen, A. Eldering, H. H. Aumann, and M. T. Chahine, 2006: Biases in total precipitable water vapor climatologies from Atmospheric Infrared Sounder and Advanced Microwave Scanning Radiometer. *J. Geophys. Res. Atmos.*, **111**, 1–14, doi:10.1029/2005JD006598.

Halbert, K. T., W. G. Blumberg, and P. T. Marsh, 2015: SHARPpy: Fueling the Python Cult. *Prepr. 5th Symp. Adv. Model. Anal. Using Python*, 1–3.

Hart, J. A., J. Whistler, R. Lindsay, and M. K., 1999: NSHARP, version 3.10. *Storm Predict. Center, Natl. Centers Environ. Predict.*,.

Stensrud, D. J., 2009: Convective-scale warn-on-forecast system. *Bull. Amer. Meteor. Soc.*, 1487–1499, doi:10.1175/2009BAMS2795.1.

Tobin, D. C., and Coauthors, 2006: Atmospheric Radiation Measurement site atmospheric state best estimates for Atmospheric Infrared Sounder temperature and water vapor retrieval validation. *J. Geophys. Res. Atmos.*, **111**, 1–18, doi:10.1029/2005JD006103.

Weisz, E., W. L. S. Sr, and N. Smith, 2013: Advances in simultaneous atmospheric profile and cloud parameter regression based retrieval from high-spectral resolution radiance measurements. *J. Geophys. Res. -Atmospheres*, **118**, 6433–6443, doi:10.1002/jgrd.50521.

9. Illustrations and Tables

PWV_QC=0 or PWV_QC=1
Cloud Fraction <= 80%
PGood >= 500 hPa
totH2OStdErr <= 19%

Table 1. AIRS quality control criteria for this study.

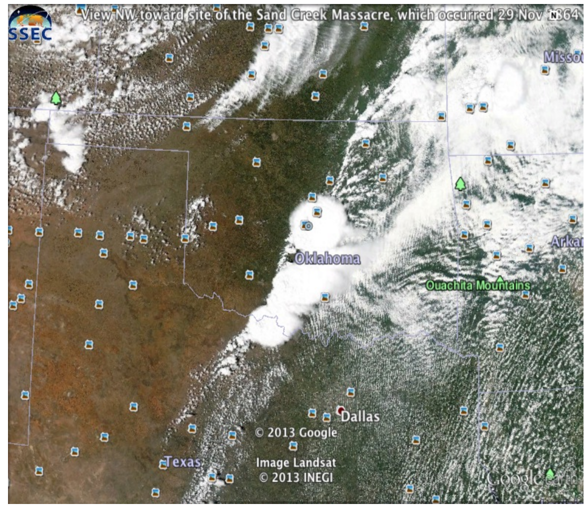

Figure 1. NASA Aqua MODIS imagery May 31, 2013 at 18:30 UTC (1:30 pm local time)

CAPE (J/kg) minimum cutoff for SONDE	ERA Mean/Std. Dev		AIRS Mean/Std. Dev	
	Surface Temperature	Surface Dew Point	Surface Temperature	Surface Dew Point
0	0.93/4.0	-0.80/4.52	1.12/3.48	0.14/4.39
50	-0.34/3.61	-2.2/3.60	-0.29/3.41	-2.11/3.64
350	-0.68/3.94	-2.72/3.75	-0.56/3.61	-2.62/3.75
820	-0.85/4.21	-3.0/3.86	-0.53/3.7	-2.67/3.91
1330	-1.02/4.61	-3.87/4.81	-0.43/2.76	-3.72/4.04
1520	-1.01/4.39	-4.33/4.29	-0.66/2.93	-4.3/4.27
2500	-1.68/4.68	-5.67/5.04	-2.28/5.94	-7.49/5.28
3050	-3.06/6.28	-5.77/7.21	-4.81/6.36	-8.36/6.54

Table 2. Error relative to ARM SGP radiosondes in surface parcel temperature and dew point temperature estimates from ERA and from AIRS using the quality control shown in Table 1.

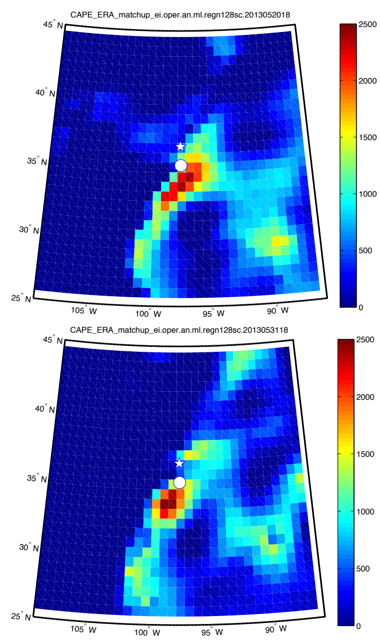

Figure 2. CAPE computed using SHARPpy from model ECMWF ERA-Interim at 18 UTC (top) and from NASA AIRS L2 v6 18:30 UTC (bottom). Circle symbol marks Norman, Oklahoma near El Reno. Star symbol marks the location of the DOE ARM SGP site.

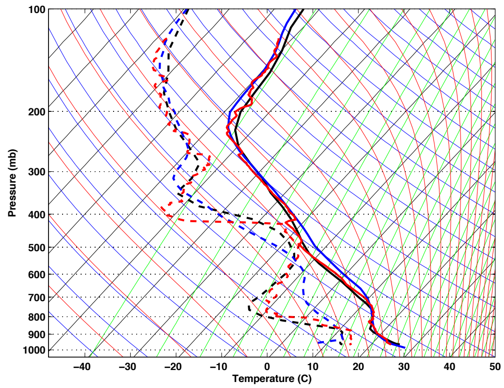

Figure 3. Temperature and dewpoint temperature vertical profiles from ARM Vaisala RS92 Radiosonde (red), ECMWF ERA-Interim (black) and NASA AIRS L2 Version 6 (blue) at the DOE ARM SGP site on 31 May 2013 at about 18:00 UTC (noon).

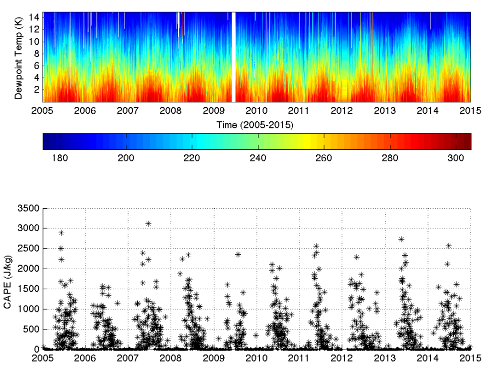

Figure 4. Seasonal variation in dewpoint (top) and surface CAPE (bottom) at the ARM SGP site.

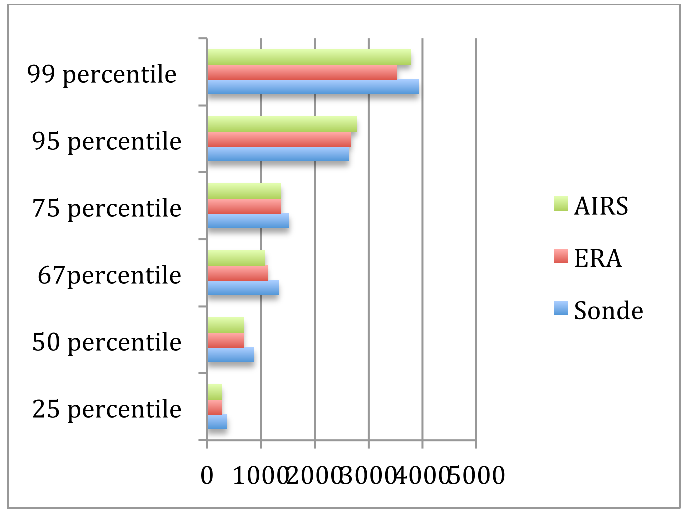

Figure 5. Southern Great Plains Cumulative Sum for 10 year climatology.

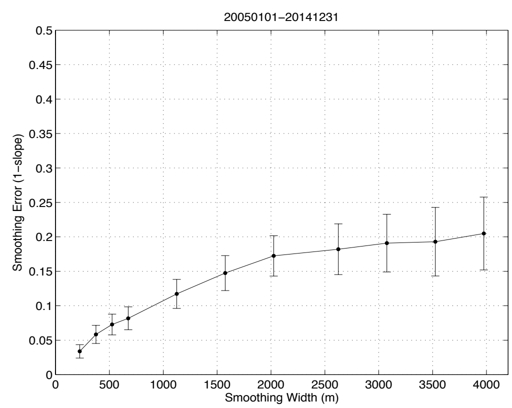

Figure 6. Vertical smoothing error by smoothing width

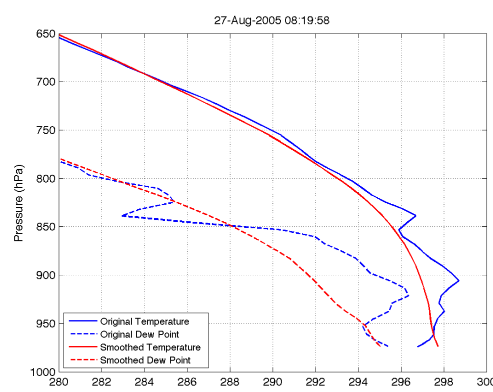

Figure 7. An example of a smoothed soundings and an original radiosonde sounding on August 27, 2005 at the ARM SGP site containing a nocturnal temperature inversion.

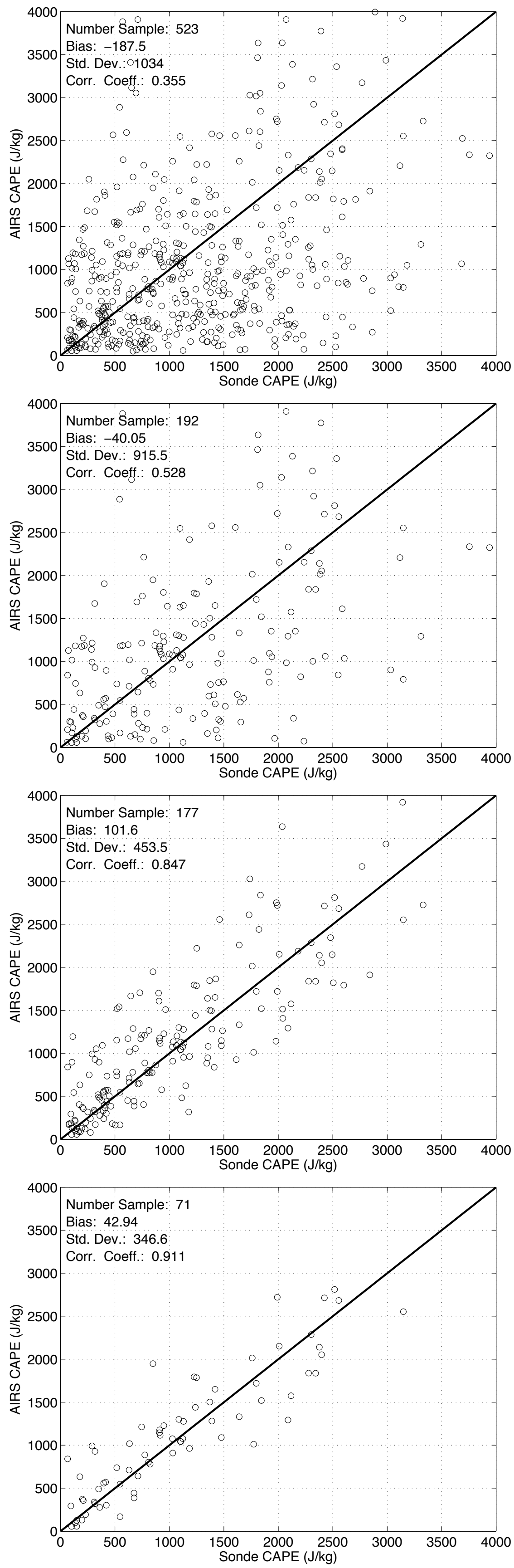

Figure 8. AIRS vs. ARM radiosonde all data with AIRS cloud fraction less than 0.8 (top) and a subset with surface dew point within one degree (second, all data with AIRS cloud fraction less than 0.1 (third) and a subset with surface dew point within one degree (bottom).

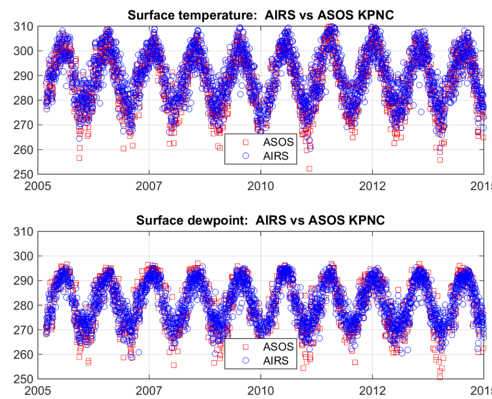

Figure 9. Two meter air temperature and dew point comparison between AIRS and the Ponca City, OK ASOS station just east of the ARM SGP site at Lamont, OK

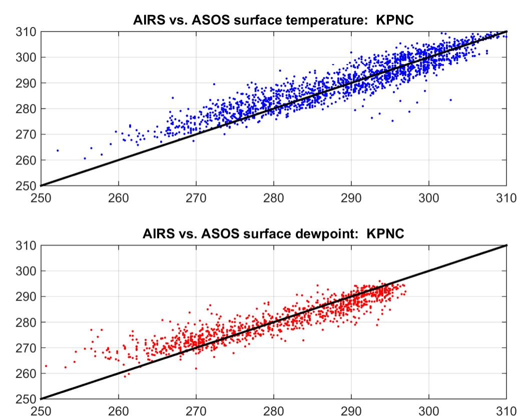

Figure 10. Scatter plot of AIRS and ASOS 2 meter temperature and dewpoint shown in Figure 9.